Materials Science in Semiconductor Processing 29 (2015) 188–192

Contents lists available at ScienceDirect

Materials Science in Semiconductor Processing

journal homepage: www.elsevier.com/locate/mssp

Influence of Sb doping on the structural, optical and electrical properties of p-ZnO thin films prepared on n-GaN/Al_2O_3 substrates by a simple CVD method

Q.J. Feng [a,*], S. Liu [a], Y. Liu [a], H.F. Zhao [b], J.Y. Lu [a], K. Tang [a], R. Li [a], K. Xu [a], H.Y. Guo [a]

[a] School of Physics and Electronic Technology, Liaoning Normal University, Dalian 116029, People's Republic of China
[b] State Key Laboratory of Luminescence and Applications, Changchun Institute of Optics, Fine Mechanics and Physics, Chinese Academy of Sciences, Changchun 130033, People's Republic of China

ARTICLE INFO

Available online 19 March 2014

Keywords:
Sb-doping
P-type ZnO
Chemical vapor deposition
Optical absorption spectrum

ABSTRACT

ZnO thin films with different Sb doping concentrations were prepared on n-GaN/Al_2O_3 substrates by simple chemical vapor deposition. Field-emission scanning electron microscopy (FE-SEM) showed that the morphologies of ZnO thin films were rougher and the size of the crystal grains reduced with increasing Sb concentration. The X-ray diffraction measurements indicated that the (002) diffraction peak positions of samples shifted gradually towards the lower angle side, which explained the substitution of Sb^{3+} into the Zn site by Sb doping. In addition, Hall measurement results indicated that Sb doped ZnO thin films had p-type conductivity, and the optimal Sb_2O_3/ZnO mass ratio for p-type ZnO thin film was approximately 1:4. Optical absorption spectrum measurement indicated that the energy gaps of the samples were evidently narrowed with increasing Sb doping concentration.

1. Introduction

ZnO is a highly promising direct wide band (E_g=3.37 eV) semiconductor material with large exciton binding energy (60 meV) at room temperature (RT) [1,2], which results in it being an excellent candidate for ultraviolet devices, such as laser diodes (LDs) [3], light emitting diodes (LEDs) [4], and photodetectors (PDs) [5]. For the growth of ZnO, the use of substrates with smaller lattice misfit would improve the quality of ZnO layers around the interface region, which consequently enables one to grow ZnO layers with improved crystallinity [6]. Many of the physical properties of GaN (a=3.189 Å, c=5.185 Å) are similar to those of ZnO (a=3.250 Å, c=5.213 Å) and they have close lattice constants [7]. Furthermore, both GaN and ZnO are wurtzite crystal structures with a similar wide band gap of 3.40 eV and 3.37 eV, respectively, at RT. That is to say, ZnO is a closely lattice-matched material to GaN with a lattice misfit of 1.8%, which is ten times smaller than that lattice misfit between ZnO and Al_2O_3 (about 18%) [8], which is normally used as a substrate for ZnO. GaN substrate is also good for device applications, because it is conductive [9]. Moreover, ZnO and GaN have a large band gap. This means that the ZnO/GaN heterostructure is a promising material for optoelectronic applications.

Furthermore, one of the biggest challenges for good ZnO-based optoelectronic devices is the difficulty of reliably fabricating p-type ZnO due to its self-compensating effect from native defects, such as oxygen vacancy (V_O), zinc interstitial (Zn_i) and H incorporation [10]. Therefore, most efforts have been focused to obtain p-type ZnO materials. Group V elements such as N [11], P [12], Sb [13], and As [14] have been tried experimentally as dopants. At present, growth techniques for ZnO thin films

* Corresponding author. Fax: +86 411 8215 8140/8503.
E-mail address: fengqiuju@163.com (Q.J. Feng).

http://dx.doi.org/10.1016/j.mssp.2014.02.031
1369-8001

have been studied, such as molecular beam epitaxy (MBE) [15], metalorganic chemical vapor deposition (MOCVD) [16], pulsed laser deposition (PLD) [17], and spin coating method [18,19]. However, there are few reports on the fabrication of p-ZnO thin films by a simple chemical vapor deposition (CVD) method. In this paper, Sb doped p-ZnO thin films were successfully prepared on n-GaN/Al_2O_3 substrates by the simple CVD method. The structural, optical and electrical properties of Sb doped ZnO thin films were investigated. And this comparatively simple method could open a relatively cheap and efficient way for fabricating ZnO based optoelectronic devices.

2. Experimental procedure

ZnO thin films with different Sb doping concentrations were grown on n-GaN/Al_2O_3 substrates by the simple CVD method. High purity metallic Zn powders (99.999%), Sb_2O_3 powders (99.99%) and oxygen gas were used as Zn, Sb and oxygen sources, respectively. Well-mixed powders of Zn and Sb_2O_3 with different weight ratios were put in a quartz boat and placed at the center of a tube furnace. The substrate was placed horizontally on the downstream side of the source at a distance of 1 cm. Fig. 1 shows the experimental set-up for the synthesis of Sb doped ZnO thin films. The whole system was pumped to a base pressure of about 10 Pa by a mechanical pump. High purity Ar carrier gas was passed at a flow rate of 100 sccm and oxygen gas was introduced into the reaction chamber at a flow rate of 30 sccm. The growth temperature in the reaction chamber was kept at 650 °C for 30 min. The growth parameters of samples with different Sb doping concentrations are listed in Table 1. The surface morphology, elemental concentration and structural properties were investigated by field-emission scanning electron microscopy (FE-SEM, HITACHI S4800), energy-dispersive spectroscopy (EDS) analysis, and X-ray diffraction (XRD) using the Cu Kα radiation, respectively. The electrical properties were measured by a Hall-effect measurement system (Bio-Rad HL5500) and the optical absorption spectra were recorded using a Shimadzu UV160 spectrometer.

3. Results and discussion

The surface morphology of samples with different Sb doping concentrations was examined by FE-SEM. As can be seen in Fig. 2, the surface morphology of undoped ZnO (sample A) is relatively smooth and it is a membranous structure composed of large single crystal mass. This indicated that high-quality ZnO thin films could be achieved by the simple CVD method. For Sb doped samples B–D, with increasing Sb concentration, the average grain size gradually decreased and had a relatively rougher surface morphology. This indicated that surfaces of the samples had become worse with the increase of Sb concentration.

EDS was used to investigate elemental concentration in the samples. As shown in Fig. 3, samples A–D consisted of zinc, oxygen, gallium, nitrogen, aluminum and antimony (in samples B–D) elements. Meanwhile antimony, zinc, and oxygen elements originated from the samples and gallium, nitrogen, and aluminum elements originated from the substrates. Furthermore, Sb concentrations in samples B, C and D were about 1%, 3% and 4%, respectively. The EDS results show that the Sb concentration in ZnO samples depends heavily on the Sb_2O_3/ZnO weight ratio of the starting powders, and therefore the Sb concentration can be controlled by this growth route.

Fig. 4 shows the XRD patterns of the samples. For comparison, n-GaN was also investigated. For low Sb doped concentration samples A–C, only ZnO (002) diffraction peak of hexagonal wurtzite structures appears as shown in Fig. 4(a). This demonstrates that high quality Sb doped ZnO thin films can be achieved by the simple CVD method. For sample D with higher Sb doping concentrations, (101) diffraction peak at 36.20° also appeared, and this observation showed that the crystalline quality became worse at high Sb doped concentrations. The results were consistent with the SEM result. Moreover, as clearly shown in Fig. 4(b), (002) diffraction peaks of samples A, B, C and D appeared at 34.51°, 34.47°, 34.45° and 34.41°, respectively. The (002) peak positions of the samples shifted toward a lower diffracting angle with increasing Sb doping concentration. This phenomenon is usually considered as change of lattice spacing caused by

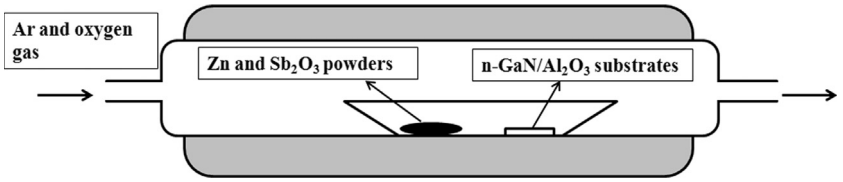

Fig. 1. Experimental set-up for the synthesis of Sb doping ZnO thin films.

Table 1
The growth parameters of the samples.

Sample	Zn (g)	Sb_2O_3 (g)	Mass ratio (Sb_2O_3/Zn)	Growth temperature (°C)	Ar (ml/min)	O_2 (ml/min)
A	0.3	0	—	650	100	30
B	0.3	0.05	1:6	650	100	30
C	0.3	0.07	1:4	650	100	30
D	0.3	0.10	1:3	650	100	30

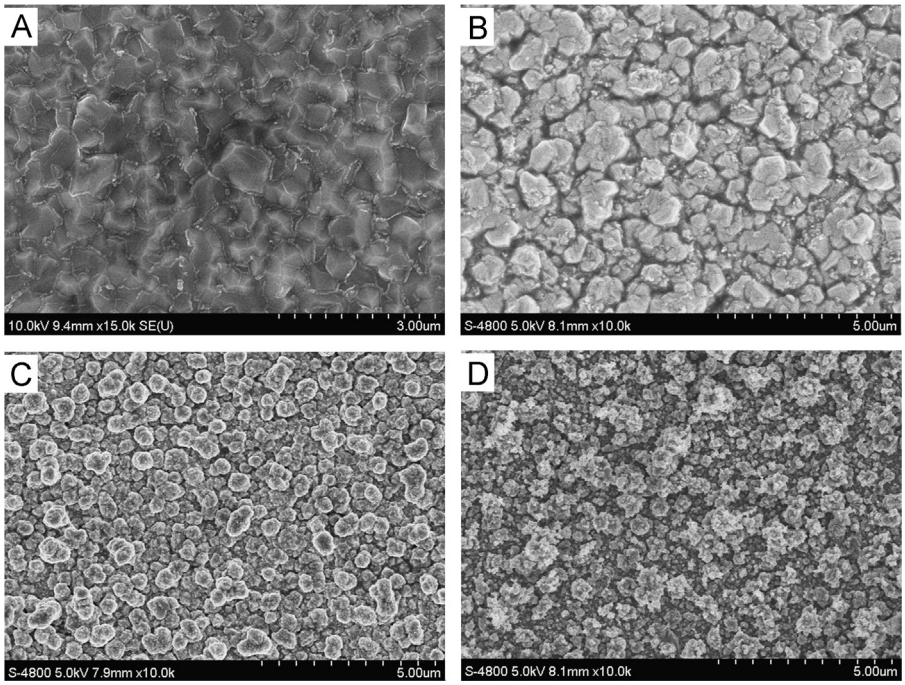

Fig. 2. FE-SEM images of samples A–D.

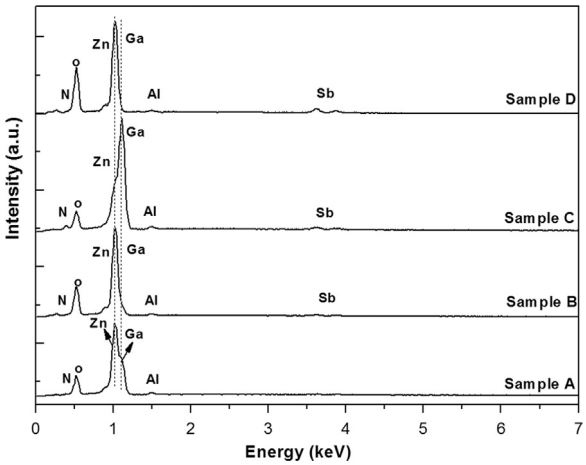

Fig. 3. EDS spectra of samples A–D.

Sb doping. The Zn^{2+} ionic radius of 0.74° is less compared to the Sb^{3+} ionic radius of 0.78° [20], which resulted in the lattice spacing becoming gradually enlarged. This explains the substitution of Sb^{3+} into the Zn site of the host ZnO.

The electrical parameters of samples as investigated by the Hall effect measurement are listed in Table 2. To eliminate the influence of the substrate on the measurement of electrical properties, undoped GaN was used. In Table 2, undoped ZnO (sample A) exhibits n-type conductivity with a resistivity of 10.10 Ω cm, and the electron concentration and hall mobility are 9.865×10^{16} cm^{-3} and 6.27 cm^2/V s, respectively. The conductivity type of the samples changed to p-type with the introduction of Sb doping. The hole concentration increased from 3.642×10^{16} cm^{-3} in sample B to 2.713×10^{17} cm^{-3} in sample C. This carrier concentration of sample C is quite close to the demand for the fabrication of ZnO based optoelectronic devices. The changes in the carrier concentrations were attributed to the fact that the Sb-related acceptor concentration was enhanced with an increasing Sb_2O_3/ZnO mass ratio, which showed that the doping concentration can be effectively controlled. The mobility decreased with increasing Sb doping concentration, which was also observed in previous work [21]. The decrease in mobility of our samples should be due to the influence of Sb impurities or Sb-induced structural defects. Moreover, with further increase in Sb doping concentration the carrier concentration decreased to 1.569×10^{16} cm^{-3} in sample D. It was because the crystalline quality of ZnO thin films became worse at a higher Sb doping concentration, which is consistent with the XRD results. The result of Hall-effect measurements also indicated that the optimal Sb_2O_3/ZnO mass ratio for achieving p-type ZnO thin films is about 1:4 by the CVD method.

The optical absorption spectra of samples A–D are shown in Fig. 5. From Fig. 5 we can see that the sharp fundamental absorption edges of samples A–D caused a distinct red-shift with increasing Sb concentration. In addition, it is generally accepted that for a material with direct band gap, the relation between $(\alpha h\nu)^2$ and photon energy $(h\nu)$ is expressed by the following formula [22]:

$$(\alpha h\nu)^2 = A(h\nu - E_g)$$

where α is the absorbance, $h\nu$ is the photon energy, A is a constant, and E_g is the optical band gap [23]. The optical band gaps (E_g) were obtained by extrapolating the linear part of the curves of $(\alpha h\nu)^2$ as a function of $h\nu$ to intercept the energy axis [24,25]. The E_g value of un-doped ZnO (sample A) is determined to be about 3.30 eV. The E_g values of sample B, C and D are 3.26 eV, 3.19 eV and

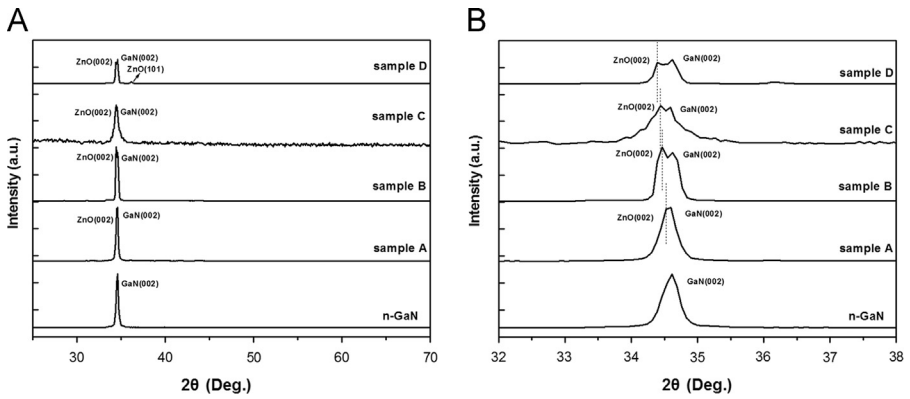

Fig. 4. (a) XRD patterns of ZnO thin films of different Sb doping concentrations and (b) the amplified pattern for (002) diffraction peaks.

Table 2
Electrical properties of ZnO thin films of different Sb concentrations.

Sample	Resistivity (Ω cm)	Mobility ($cm^2/V\,s$)	Carrier concentration (cm^{-3})	Conductivity type
A	10.10	6.27	9.865×10^{16}	n
B	35.34	4.85	3.642×10^{16}	p
C	24.27	0.95	2.713×10^{17}	p
D	67.61	5.89	1.569×10^{16}	p

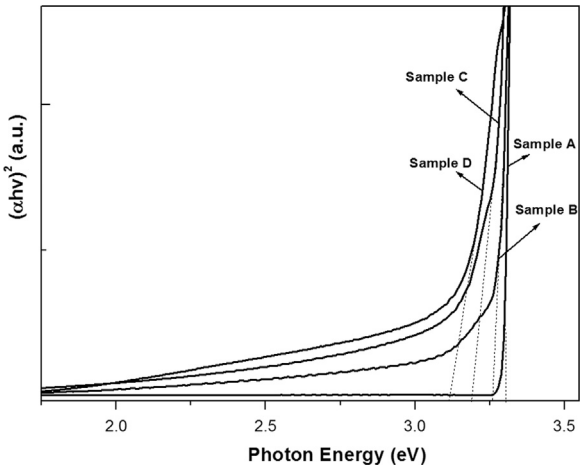

Fig. 5. $(\alpha h\nu)^2$ vs. $(h\nu)$ plot of samples A–D.

3.11 eV, respectively. It can be seen that E_g values show an evident narrowing with increasing Sb doping concentration. The detailed explanations for this band gap narrowing are unfeasible at present, but according to previous reports, we can consider that Sb doping can introduce an acceptor energy level and the acceptor binding energies are at 160 and 130–140 meV [26]. Therefore, the shrinkage of E_g in the absorption spectra should be partly attributed to the band-tailing effect introduced by Sb doping.

In order to further investigate the optical behavior of Sb doped ZnO thin films, low-temperature (10 K) PL spectra of undoped ZnO and p-type ZnO were examined, as shown in Fig. 6. The PL spectra of undoped ZnO and sample B show a strong near-band-edge emission peak located at

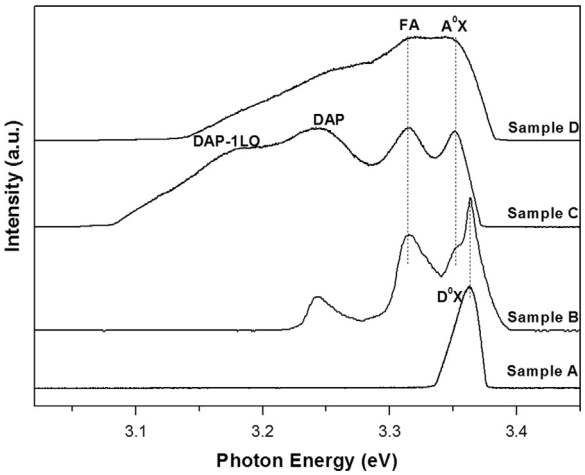

Fig. 6. The photoluminescence spectra of samples A–D at 10 K.

3.363 eV, which is assigned to the transition of neutral donor-bound exciton (D^0X) [27]. In the spectra of samples C and D, the D^0X disappeared. Furthermore, in samples B, C and D, four new emissions peaks located at 3.353, 3.314, 3.244, and 3.172 eV were observed. The PL peak located at 3.353 eV was assigned to a neutral acceptor bound exciton (A^0X) [28,29]. The band at 3.314 eV is attributed to the recombination emissions between free electrons and acceptor holes (FA) [21,28]. The peak position at 3.244 eV was attributed to the donor–acceptor pair (DAP) emission [30]. For sample C, we note that the peaks at 3.244 and 3.172 eV have equal energy spacing of 72 meV, which is in good agreement with the energy of LO phonons of ZnO. This implies that the peak at 3.172 eV is the corresponding first LO phonon peak of the DAP.

4. Conclusions

Sb doped p-type ZnO thin films were successfully prepared on n-GaN/Al_2O_3 substrates by the simple CVD method. The influence of Sb doping on the structural, optical and electrical properties of the ZnO thin films was studied. The results explained that the morphology of the samples was relatively rougher and the grain size showed

a gradual decrease with increasing Sb concentration, and the XRD pattern analysis indicated the substitution of Sb^{3+} into the Zn site of the host ZnO. At the same time, the energy gaps of ZnO thin films showed an evident narrowing by Sb doping. Furthermore, we also obtained results which indicated that the optimal Sb_2O_3/ZnO mass ratio was approximately 1:4 for the p-type ZnO thin film prepared by the simple CVD method. This proposed method provides a way of realizing cheap and efficient ZnO based optoelectronic devices.

Acknowledgments

This work was supported by the NSFC (Grant nos. 10804040, 11004020, and 11004092), the Doctoral Scientific Research Starting Foundation of Liaoning province (No. 20101061), the Nature Science Foundation of Dalian City (No. 2010J21DW020), the Key Laboratory of Space Laser Communication and Testing Technology, Chinese Academy of Sciences (KJJG10-1).

References

[1] Vrushali Shelke, M.P. Bhole, D.S. Patil, Mater. Chem. Phys. 141 (2013) 81–88.
[2] Vrushali Shelke, M.P. Bhole, D.S. Patil, J. Alloys Compd. 572 (2013) 68–73.
[3] D.C. Look, B. Claflin, Phys. Status Solidi B 241 (2004) 624–630.
[4] P.C. Tao, Q.J. Feng, J.Y. Jiang, H.F. Zhao, R.Z. Xu, S. Liu, M.K. Li, J.C. Sun, Z. Song, Chem. Phys. Lett. 522 (2012) 92–95.
[5] C. Soci, A. Zhang, B. Xiang, S.A. Dayeh, D.P.R. Aplin, J. Park, X.Y. Bao, Y.H. Lo, D. Wang, Nano Lett. 7 (4) (2007) 1003–1009.
[6] S.K. Hong, H.J. Ko, Y.F. Chen, T. Hanada, T. Yao, J. Cryst. Growth 214–215 (2000) 81–86.
[7] B.J. Zhao, H.J. Yang, G.T. Du, G.Q. Miao, Y.T. Zhang, Z.M. Gao, T.P. Yang, J.Z. Wang, W.C. Li, Y. Ma, X.T. Yang, B.Y. Liu, D.L. Liu, X.J. Fang, J. Cryst. Growth 258 (2003) 130–134.
[8] H.J. Ko, Y.F. Chen, S.K. Hong, T. Yao, J. Cryst. Growth 209 (2000) 816–821.
[9] D.C. Oh, T. Suzuki, J.J. Kim, H. Makino, T. Hanada, M.W. Cho, T. Yao, J.S. Song, H.J. Ko, J. Vac. Sci. Technol. B 23 (2005) 1281–1285.
[10] G.P. Wang, S. Chu, N. Zhan, Y.Q. Lin, L. Chernyak, J.L. Liu, Appl. Phys. Lett. 98 (2011) 041107.
[11] D. Wang, J.W. Zhang, Y.P. Peng, Z. Bi, X.M. Bian, X.A. Zhang, X. Hou, J. Alloys Compd. 478 (2009) 3225–3329.
[12] B. Xiang, P.W. Wang, X.Z. Zhang, S.A. Dayeh, D.P.R. Aplin, C Soci, Dapeng Yu, D. Wang, Nano Lett. 7 (2007) 323–328.
[13] T. Yang, B. Yao, T.T. Zhao, G.Z. Xing, H. Wang, H.L. Pan, R. Deng, Y.R. Sui, L.L. Gao, H.Z. Wang, T. Wu, D.Z. Shen, J. Alloys Compd. 509 (2011) 5426–5430.
[14] Q.J. Feng, L.Z. Hu, H.W. Liang, Y. Feng, J. Wang, J.C. Sun, J.Z. Zhao, M.K. Li, L. Dong, Appl. Surf. Sci. 257 (2010) 1084–1087.
[15] X.A. Zhang, J.W. Zhang, W.F. Zhang, D. Wang, Z. Bi, X.M. Bian, X. Hou, Thin Solid Films 516 (2008) 3305–3308.
[16] J.F. Su, C.Q. Wang, C.J. Tang, Q. Niu, Y.S. Zhang, Z. Fu, J. Alloys Compd. 509 (2011) 6102–6105.
[17] S.K. Lee, J.Y. Son, Appl. Phys. Lett. 100 (2012) 132109.
[18] Vrushali Shelke, B.K. Sonawane, M.P. Bhole, D.S. Patil, J. Non-Cryst. Solids 355 (2009) 840–843.
[19] B.K. Sonawane, M.P. Bhole, D.S. Patil, Opt. Quantum Electron. 41 (2009) 17–26.
[20] K. Samanta, P. Bhattacharya, R.S. Katiyar, J. Appl. Phys. 108 (2010) 113501.
[21] J.Z. Zhao, H.W. Liang, J.C. Sun, Q.J. Feng, J.M. Bian, Z.W. Zhao, H.Q. Zhang, L.Z. Hu, G.T. Du, Electrochem. Solid-State Lett. 11 (2008) 323–326.
[22] W.W. Zhong, F.M. Liu, L.G. Cai, C.C. Zhou, P. Ding, H. Zhang, J. Alloys Compd. 499 (2010) 265–268.
[23] S. Ilican, Y. Caglar, M. Caglar, F. Yakuphanoglu, J.B Cui, Physica E 41 (2008) 96–100.
[24] Y.Z. Zhang, J.G. Lu, Z.Z. Ye, H.P. He, L.P. Zhu, B.H. Zhao, L. Wang, Appl. Surf. Sci. 254 (2008) 1993–1996.
[25] Q.J. Feng, D.Z. Shen, J.Y. Zhang, Y.M. Lu, Y.C. Liu, X.W. Fan, Mater. Chem. Phys. 96 (2006) 158–162.
[26] J.Z. Zhao, H.W. Liang, J.C. Sun, Q.J. Feng, S.S. Li, J.M. Bian, L.Z. Hu, G.T. Du, J.J. Ren, J.L. Liu, Phys. Status Solidi A 208 (2011) 825–828.
[27] C.H. Zang, D.X. Zhao, Y. Tang, Z. Guo, J.Y. Zhang, D.Z. Shen, Y.C. Liu, Chem. Phys. Lett. 452 (2008) 148–151.
[28] H.Q. Zhang, L.Z. Hu, Z.W. Zhao, J.X. Ma, Y. Qiu, B. Wang, H.W. Liang, J.M. Bian, Vacuum 85 (2011) 718–720.
[29] K. Samanta, A.K. Arora, S. Hussain, S. Chakravarty, R.S. Katiyar, Curr. Appl. Phys. 12 (2012) 1381–1385.
[30] X. Fang, J.H. Li, D.X. Zhao, B.H. Li, Z.Z. Zhang, D.Z. Shen, X.H. Wang, Z.P. Wei, Thin Solid Films 518 (2010) 5687–5689.